Rspo2 antagonizes FGF signaling during vertebrate mesoderm formation and patterning

Alice H. Reis and Sergei Y. Sokol

Department of Cell, Developmental and Regenerative Biology,
Icahn School of Medicine at Mount Sinai, New York

*Correspondence: Sergei Y. Sokol, Ph. D.,
Phone: 1-212-241-1757; Fax: 1-212-860-9279
E-mail: sergei.sokol@mssm.edu

Summary

R-spondins are a family of secreted proteins that play important roles in embryonic development and cancer. R-spondins have been shown to modulate the Wnt pathway, however their involvement in other developmental signaling processes have remained largely unstudied. Here we describe a novel function of Rspo2 in FGF pathway regulation *in vivo*. Overexpressed Rspo2 inhibited elongation of *Xenopus* ectoderm explants and Erk1 activation in response to FGF. By contrast, the constitutively active form of Mek1 stimulated Erk1 even in the presence of Rspo2, suggesting that Rspo2 functions upstream of Mek1. The observed inhibition of FGF signaling was accompanied by the dowregulation of the FGF target genes *tbxt/brachyury* and *cdx4* that mediate anterioposterior axis specification. Importantly, these target genes were upregulated in Rspo2-depleted explants. The FGF inhibitory activity was mapped to the thrombospondin type 1 region (TSP), contrasting the known function of the Furin-like domains (FU) in Wnt signaling. Further domain analysis revealed an unexpected intramolecular interaction that may control Rspo2 signaling output. We conclude that, in addition to its role in Wnt signaling, Rspo2 acts as an FGF antagonist during mesoderm formation and patterning. ;

Introduction

R-spondins are a family of four highly conserved secreted proteins (Rspo1-4) that play critical roles during embryonic development and cancer (Aoki et al., 2007; de Lau et al., 2014; Kim et al., 2006; Raslan and Yoon, 2019). Mouse embryos lacking *rspo2,* encoding an R-spondin that is abundant in early embryogenesis, do not survive to term due to lung, limb, and craniofacial defects (Aoki et al., 2008; Bell et al., 2008; Nam et al., 2007; Yamada et al., 2009). Rspo2 has been also implicated in skeletogenesis (Tatsumi et al., 2014) and muscle development (Kazanskaya et al., 2004). Besides embryonic development, R-spondins are involved in stem cell survival (Kim et al., 2005; Sato et al., 2009) and multiple cancers. About 10% of colorectal tumors were discovered to contain gene fusions involving *rspo2* and *rspo3*, these fusions were mutually exclusive with APC mutations (Seshagiri et al., 2012). Rspo2 has been also reported to modulate mammary tumorigenesis (Lowther et al., 2005; Theodorou et al., 2007). These observations highlight the important functions of R-spondins, and specifically Rspo2, during early development and disease.

R-spondins functions have been mostly attributed to their ability to promote Wnt signaling (Bell et al., 2008; de Lau et al., 2014; Jin and Yoon, 2012; Kazanskaya et al., 2004). R-spondins upregulate Wnt signaling by preventing Frizzled receptor degradation when in complex with LGR4/5 and RNF43/ZNRF3 (Carmon et al., 2011; de Lau et al., 2011; Hao et al., 2012; Koo et al., 2012). R-spondins share a highly conserved structure comprised of a signal peptide followed by two furin-like domains (FU1 and FU2), thrombospondin type 1 domain (TSP) and a C-terminal region enriched in basic amino acids (BR) (Jin and Yoon, 2012; Kim et al., 2006). The effect of R-spondins on the Wnt/β-catenin pathway has been attributed to the furin-like domains, whereas the TSP domain of Rspo3 has been shown to bind Syndecan4 and modulate non-canonical Wnt signaling (Ohkawara et al., 2011). The interaction of R-spondins with other signaling pathways remains poorly understood.

Several arguments suggest that the FGF pathway may be regulated by R-spondins. First, Rspo3 overexpression in *Xenopus* embryos produces blastopore closure defects (Ohkawara et al., 2011), mimicking the effect of a dominant interfering FGF receptor (Amaya et al., 1991). Second, the TSP domain of Rspo3 interacts with syndecans and glypicans (Ohkawara et al., 2011), heparan sulfate proteoglycans (HSPGs) that function as coreceptors for FGF (Garcia-Garcia and Anderson, 2003; Rapraeger et al., 1991; Yayon et al., 1991). Third, the mouse embryos lacking the functions of FGF antagonists Spry2 and Spry4 (Taniguchi et al., 2007) exhibit similar defects as Rspo2–deficient embryos (Aoki et al., 2008; Bell et al., 2008; Nam et al., 2007; Yamada et al., 2009). Finally, Rspo3 knockdown upregulated Erk1 phosphorylation after osteogenic differentiation of human adipose-derived stem cells (Zhang et al., 2017). Together, these observations indicate that R-spondins may play a role in FGF signaling, in addition to their known function as Wnt modulators.

FGF signaling is initiated with the binding of the ligand to the tyrosine kinase receptors FGFR1-4. Tyrosine kinase stimulation leads to an intracellular signal transduction cascade that includes the activation of Ras and a series of cytosolic kinases including Raf, Mek and Erk, ultimately leading to target gene transcription (Ornitz and Itoh, 2015; Patel and Shvartsman, 2018). Different FGF ligands have been shown to function in early mesoderm induction and CNS posteriorization, limb, lung, heart, among other tissues, in vertebrate embryos and have been implicated in cancer (Belov and Mohammadi, 2013; Ornitz and Itoh, 2015; Turner and Grose, 2010). In early embryogenesis, the FGF pathway is known to function in gastrulation and anteroposterior axis specification (Dorey and Amaya, 2010).

Taken together, this evidence prompted us to investigate whether Rspo2 has a role in FGF signaling during vertebrate embryonic develoment. We used *Xenopus* early embryos, in which Rspo2 is abundantly expressed in the marginal zone during

gastrulation and may therefore regulate FGF signaling during mesoderm formation (Kimelman and Kirschner, 1987; Slack et al., 1987). We show that Rspo2 inhibits FGF-mediated mesoderm specification and posterior patterning. These antagonistic effects of Rspo2 are mediated by the TSP domain upstream of the FGF receptors. Based on our analysis, we further propose that this inhibitory activity is modulated by an intramolecular interaction in Rspo2.

Results and Discussion

Rspo2 blocks FGF signaling

Microinjection of Rspo2 RNA into two dorsal blastomeres of four-cell *Xenopus* embryos produced blastopore closure defects and subsequent tail truncations that were reminiscent of the phenotype obtained with a dominant interfering mutant of the FGF receptor 1 (Amaya et al., 1991)(**Fig. S1**), suggesting that Rspo2 may antagonize the FGF pathway. To investigate whether Rspo2 can modulate FGF signaling, we assessed mesoderm induction in ectoderm explants treated with FGF2 (Kimelman and Kirschner, 1987; Slack et al., 1987). Upon FGF2 stimulation, these explants acquire mesodermal cell fates and undergo extensive morphogenetic movements that are characteristic of mesoderm during gastrulation. We observed that control explants developed as expected into atypical epidermis, while FGF2-treated explants have elongated by the time correspondent to the end of gastrulation (**Fig. 1A-B**). The injection of Rspo2 RNA prevented explant elongation (**Fig.1C**). In the absence of FGF2, the morphology of the Rspo2-expressing explants was indistinguishable from untreated control explants (**Fig.1D**). These observations indicate that Rspo2 prevented the elongation response of the cells to FGF2. Furthermore, Rspo2 inhibited FGF-dependent phosphorylation of Erk1, a downstream signaling target (LaBonne et al., 1995; Umbhauer et al., 1995) **(Fig. 1E)**. These findings demonstrate that Rspo2 is a negative regulator of FGF2 signaling.

To determine which level of the FGF pathway is affected by Rspo2, we asked whether Rspo2 inhibits the effect of the active form of Mek1 (Mek1^{CA}), an upstream activator of Erk1 (Cowley et al., 1994; Umbhauer et al., 1995). Mek1^{CA} upregulated Erk1 phosphorylation even in the presence of Rspo2, suggesting that Rspo2 functions upstream of Mek1 (**Fig. 1F**).

Finally, we evaluated the expression of *tbxt/brachyury*, a direct FGF target gene (Smith et al., 1991), in FGF2-stimulated ectoderm explants. RT-qPCR demonstrated that *tbxt* expression has been strongly inhibited by Rspo2 by stage 13. (**Fig. 1G**). Taken together, these results show that Rspo2 is an efficient antagonist of FGF signaling.

Enhanced FGF signaling in embryos deficient in Rspo2 function

Since overexpressed Rspo2 inhibited FGF signaling in our experiments, we predicted that, conversely, Rspo2 loss-of-function should stimulate the FGF pathway. To test this possibility, we designed and validated a specific morpholino oligonucleotide (RMO^ATG) (Heasman et al., 2000) (**Fig. S2A**). Rspo2 is known to be expressed in the marginal zone that produces FGF-dependent mesoderm, consistent with Rspo2 being induced by FGF (Kazanskaya et al., 2004). Ectoderm explants were dissected from stage 8 control embryos or embryos injected with 10 ng of RMO^ATG. After stimulation with FGF2, we observed that Rspo2-depleted explants elongated more efficiently than the control FGF2-treated explants (**Fig. 2A, B**). The morphology of the Rspo2-depleted explants did not change. This result implies that the response of Rspo2-depleted cells to FGF is enhanced. Further supporting this conclusion, RT-qPCR showed an increase in the expression of *tbxt* in FGF-treated explants as compared to the controls (**Fig. 2C**).

We also assessed a role for Rspo2 in the regulation of another FGF target gene, *cdx4/Xcad3* (Northrop and Kimelman, 1994) and *mesogenin1/msgn1* (Wittler et al., 2007) in the context of endogenous FGF signaling. RT-qPCR was performed for uninjected control or Rspo2-depleted dorsal marginal zone explants, in the absence of exogenous FGF. RMO^ATG upregulated *cdx4* and *msgn1* transcript levels as compared to controls (**Fig. 2D, E**). The same conclusion has been reached with an independent splice-blocking morpholino (RMO^SB) **(Figs. 2D, E and Fig. S2B)**. Wholemount *in situ* hybridization also confirmed the upregulation of the *cdx4* expression domain in Rspo2 morphants (**Fig. 2F**). Embryos injected with either MO developed head truncations (Fig. 2G), consistent with FGF-mediated

posteriorization. This phenotype is complementary to the posterior defects of embryos with overexpressed Rspo2. Together, these findings indicate that Rspo2 antagonizes FGF signaling during mesoderm patterning. Consistent with this conclusion, Rspo3 shRNA upregulated Erk1 phosphorylation after 14-day osteogenic differentiation of human adipose-derived stem cells, however, the direct effect of Rspo3 on FGF signaling has not been evaluated (Zhang et al., 2017).

The TSP domain mediates the FGF inhibitory activity of Rspo2

We next sought to determine which Rspo2 domain mediates FGF inhibition. Several deletion constructs that include different Rspo2 domains have been made and tested for the ability to interfere with FGF signaling in ectoderm explants (**Fig. 3A).** When introduced into early embryos, these constructs were all expressed at comparable levels (**Fig. S3**). Overexpression of Rspo2, RspoΔF or RspoΔT did not alter explant morphology on their own. However, upon FGF stimulation, Rspo2 and RspoΔF blocked explant elongation, indicating that the presence of the TSP domain correlates with the inhibitory activity (**Fig. 3B-H**). Unexpectedly, RspoΔT strongly enhanced the elongation (**Fig. 3I**), suggesting that it might have a dominant interfering effect.

In agreement with the phenotypic analysis, Rspo2 and RspoΔF reduced Erk1 phosphorylation, while RspoΔT increased it (**Fig. 3J**). We next used SU5402, an specific inhibitor of FGF receptor activity (Fletcher and Harland, 2008; Mohammadi et al., 1997), to test whether the effects of RspoΔT on Erk1 require FGF receptor. Indeed, SU5402 inhibited Erk1 phosphorylation caused by FGF2 in the presence of RspoΔT. This result is consistent with the effect of RspoΔT upstream or parallel to the FGF receptor.

To ensure that Rspo2 is a specific antagonist of the FGF pathway, we tested wheteher it would interfere with Activin/Nodal/Smad2 pathway activation. Stimulation of ectoderm explants with Activin A resulted in Smad2 phosphorylation, that was not altered by overexpressed Rspo2, RspoΔF or RspoΔT (**Fig. S4**).

Taken together, our experiments identify TSP as the domain responsible by the inhibitory effect of Rspo2 on FGF signaling.

Rspo domain interactions

In order to understand how the TSP domain blocks FGF signaling, we first asked whether RspoΔF or Rspo2 would interact with FGFR1. Our immunoprecipitation experiments did not show an interaction between these molecules (data not shown). Since RspoΔT upregulated animal cap elongation and Erk1 activation in response to FGF, i. e. exhibited an effect opposite to the one in TSP, we next hypothesized that TSP activity is masked in Rspo2 by another protein domain. To test this possibility, two-cell embryos were co-injected with RspoΔF-GFP and RspoΔT-Flag RNAs. Co-immunoprecipitation analysis revealed the binding of RspoΔF-GFP to RspoΔT-Flag (**Fig. 4A**). Moreover, full length Rspo-GFP also associated with RspoΔT-Flag (**Fig. 4B**), indicating that both intra- and intermolecular interactions may contribute to Rspo2 signaling. Currently, we cannot exclude the potential contribution of the C terminus retained in our constructs to the observed interaction.

These experiments reveal a novel domain interaction in Rspo2 that may modulate its biological activity through an additional layer of regulation. This interaction allows us to propose that RspoΔT has a dominant interfering effect by binding to endogenous inhibitory TSP domains. Alternatively, the synergy of RspoΔT with FGF might be due to RspoΔT interaction with other signaling pathways, e. g. Activin/Nodal or Wnt signaling. So far we found no evidence for RspoΔT influencing Smad2 phosphorylation in response to Activin (**Fig. S4**). However, RspoΔT may cooperate with FGF by promoting Wnt signaling, consistent with the reported synergy of FGF and Wnt proteins (Christian et al., 1992). In support of this hypothesis, Rspo2 has been demonstrated to stimulate Wnt signaling via its FU-like domains (preserved in RspoΔT) by interfering with ZNRF3/RNF43, an inhibitor of Wnt signaling (Hao et al., 2012; Koo et al., 2012).

In addition to the previously studied role of R-spondins in Wnt signaling (Bell et al., 2008; de Lau et al., 2014; Jin and Yoon, 2012; Kazanskaya et al., 2004), this work

demonstrates that Rspo2 acts as an antagonist of the FGF pathway during early embryonic development. At present, the mechanism underlying this function of Rspo2 remains unclear. Whereas the modulation of Wnt signaling by R-spondins involves the FU domains (Carmon et al., 2011; de Lau et al., 2011; Hao et al., 2012; Koo et al., 2012), the inhibitory activity of Rspo2 in FGF signaling is mediated by the TSP domain. So far, we could not detect any physical association of TSP with FGF ligands and receptors (data not shown). We propose that TSP inhibits FGF by sequestering HSPGs, essential FGF coreceptors (Rapraeger et al., 1991; Yayon et al., 1991) (**Fig. 4C**). In support of this possibility, both Rspo2 and Rspo3 have been reported to bind Syndecan4 and Glypican3 (Ohkawara et al., 2011). Further studies are needed to clarify the Rspo2 role in the FGF pathway.

Methods

Plasmids, in vitro RNA synthesis and morpholino oligonucleotides.

The DNA clone 6988843 encoding *X. tropicalis* Rspo2 was obtained from Dharmacon. The plasmids for expression of Rspo2 (pCS2-Rspo2-Flag or pCS2-Rspo2-Flag-GFP) was generated by inserting the coding region of Rspo2 sequence amplified by PCR into the EcoRI and BamHI sites of pCS2-Flag or pCS2-Flag-GFP. Deletion mutants of Rspo2 (**Table S1**) constructs were generated using single primer-based site-directed mutagenesis as described (Itoh et al., 2005). pCS2-RspoΔF-Flag and pCS2-RspoΔF-GFP lacks amino acids 37-134. pCS2-RspoΔT-Flag and pCS2-RspoΔT-GFP lacks amino acids 147-204. All constructs were verified by Sanger sequencing. Details of cloning are available upon request. pCS2-Mek^{CA} was a gift from Stanislav Shvartsman.

Capped mRNAs were synthesized using mMessage mMachine kit (Ambion, Austin, TX). The following linearized plasmids have been used as templates: pCS2-Rspo-Flag, pCS2-Rspo-Flag-GFP, pCS2-RspoΔF-Flag, pCS2-RspoΔF-GFP, pCS2-RspoΔT-Flag, pCS2-Mek^{CA}.

The following MOs were purchased from Gene Tools (Philomath, OR): RspoMO^{ATG}, 5'- AAAGAGTTGAAACTGCATTTGG -3', RspoMO^{SB}, 5'-GCAGCCTGGATACACAGAAACAAGA-3', control MO (CoMO), 5'-GCTTCAGCTAGTGACACATGCAT-3'.

Xenopus embryo culture, microinjections, imaging and statistical analysis.

 In vitro fertilization and culture of *Xenopus laevis* embryos were carried out as previously described (Dollar et al., 2005). Frog handling was according to the animal protocol approved by the MSSM IACUC. Staging was according to Nieuwkoop and Faber (Nieuwkoop and Faber, 1967). For microinjections, four-cell embryos were transferred into 3 % Ficoll in 0.5x Marc's Modified Ringer's (MMR) buffer (50 mM NaCl, 1 mM KCl, 1 mM $CaCl_2$, 0.5 mM $MgCl_2$, 2.5 mM HEPES pH 7.4) (Peng, 1991) and 10 nl of mRNA or MO solution (10 ng of $RspoMO^{ATG}$ and 20 ng of $RspoMO^{SB}$) was injected into one or more blastomeres. Control MO was injected as at a dose that matched the highest dose of RspoMO used in the same experiment. Amounts of injected mRNA and MOs have been optimized in preliminary dose-response experiments. Embryos were imaged at the indicated stages using Leica Wild M10 stereomicroscope using the OpenLab software. Unless otherwise specified, all experiments were carried out at least three times. Statistical analyses were performed using GraphPad Prism 6 software. Error bars represent as the mean +/- s. d. and Student's *t*-test was used to determine statistical significance (*$p<0.05$; **$p<0.01$).

Ectoderm and marginal zone explants, RT-qPCR

Two-to-four cell embryos were injected animally with Rspo2 RNA (0.5 ng). At stage 8 the ectodermal explants were dissected and treated with recombinant FGF2 at 25-100 ng/ml as described (Itoh and Sokol, 1994). SU5402 was added to the medium at 100 µM concentration, according to Fletcher and Harland (2008). The explants were cultured until early neurula stage, when they were analyzed for morphology, harvested for western blot or RT-qPCR. Marginal zone explants were dissected at early gastrula stage and cultured until stage 12.5 when they were lysed for RT-qPCR analysis.

For quantitative PCR (RT-qPCR), RNA was extracted from a group of ten animal caps or seven marginal zone explants at stages 12.5, using RNeasy kit (Qiagen). cDNA was made from 1 µg of total RNA using iScript (Bio-Rad). qPCR reactions were amplified using a CFX96 light cycler (Bio-Rad) with Universal SYBR Green Supermix (Bio-Rad). Data represent at least 3 independent experiments made in

triplicates. Means +/- s. d. are shown. All samples were normalized to e*ef1a1* expression and marker expression in control embryos.   Primer sequences used for RT-qPCR are listed in **Table S1**.

For Activin A treatment, ectodermal explants were dissected at stage 8 and stimulated with 0.5 ng/ml of recombinant Activin A (Itoh and Sokol, 1994) for 30 min. Cell lysates were separated by PAGE and immunoblotted with anti-phospho-Smad2 (1:1000, 3108, Cell Signaling) and anti-Flag antibody.

Immunoprecipitation and immunoblot analysis, wholemount in situ hybridization.

Immunoprecipitation was performed by using 30 embryos per condition. Embryos were injected at four-cell stage with Rspo-ΔF-GFP, Rspo-ΔT-Flag or Rspo-Flag-GFP RNA. Embryos were lysed at stage 11 and GFP pulldown was carried out by incubating the lysates with GFP-Trap (Chromotek) according to the manufacturer instructions. Immunoblot analysis was carried out as described (Itoh et al., 2005). Briefly, 10 animal caps cultured until the equivalent of stage 13 were homogenized in 50 µl of the lysis buffer (50 mM Tris-HCl pH 7.6, 50 mM NaCl, 1 mM EDTA, 1% Triton X-100, 10 mM NaF, 1 mM Na_3VO_4, 25 mM β-glycerol phosphate, 1 mM PMSF). After centrifugation for 3 min at 16000 g, the supernatant was subjected to SDS-PAGE and immunoblotting. The following primary antibodies were used: mouse anti-FLAG (M2, Sigma), mouse anti-GFP (SC-9996, Santa Cruz), rabbit anti-phospho-p44/42 MAPK (pErk1/2) (4370S, Cell Signaling). Staining with rabbit anti-Erk1 (SC-94, Santa Cruz) was used as loading control. Chemiluminescence was captured by the ChemiDoc MP imager (BioRad).

Whole-mount in situ hybridization was carried out using standard techniques (Harland, 1991) with the digoxigenin-labeled antisense RNA probes for *cdx4* (Northrop and Kimelman, 1994).

References

Amaya, E., Musci, T. J. and Kirschner, M. W. (1991). Expression of a dominant negative mutant of the FGF receptor disrupts mesoderm formation in Xenopus embryos. *Cell* **66**, 257-270.

Aoki, M., Kiyonari, H., Nakamura, H. and Okamoto, H. (2008). R-spondin2 expression in the apical ectodermal ridge is essential for outgrowth and patterning in mouse limb development. *Dev Growth Differ* **50**, 85-95.

Aoki, M., Mieda, M., Ikeda, T., Hamada, Y., Nakamura, H. and Okamoto, H. (2007). R-spondin3 is required for mouse placental development. *Dev Biol* **301**, 218-226.

Bell, S. M., Schreiner, C. M., Wert, S. E., Mucenski, M. L., Scott, W. J. and Whitsett, J. A. (2008). R-spondin 2 is required for normal laryngeal-tracheal, lung and limb morphogenesis. *Development* **135**, 1049-1058.

Belov, A. A. and Mohammadi, M. (2013). Molecular mechanisms of fibroblast growth factor signaling in physiology and pathology. *Cold Spring Harb Perspect Biol* **5**.

Carmon, K. S., Gong, X., Lin, Q., Thomas, A. and Liu, Q. (2011). R-spondins function as ligands of the orphan receptors LGR4 and LGR5 to regulate Wnt/beta-catenin signaling. *Proc Natl Acad Sci U S A* **108**, 11452-11457.

Christian, J. L., Olson, D. J. and Moon, R. T. (1992). Xwnt-8 modifies the character of mesoderm induced by bFGF in isolated Xenopus ectoderm. *Embo J* **11**, 33-41.

Cowley, S., Paterson, H., Kemp, P. and Marshall, C. J. (1994). Activation of MAP kinase kinase is necessary and sufficient for PC12 differentiation and for transformation of NIH 3T3 cells. *Cell* **77**, 841-852.

de Lau, W., Barker, N., Low, T. Y., Koo, B. K., Li, V. S., Teunissen, H., Kujala, P., Haegebarth, A., Peters, P. J., van de Wetering, M., et al. (2011). Lgr5 homologues associate with Wnt receptors and mediate R-spondin signalling. *Nature* **476**, 293-297.

de Lau, W., Peng, W. C., Gros, P. and Clevers, H. (2014). The R-spondin/Lgr5/Rnf43 module: regulator of Wnt signal strength. *Genes Dev* **28**, 305-316.

Dollar, G. L., Weber, U., Mlodzik, M. and Sokol, S. Y. (2005). Regulation of Lethal giant larvae by Dishevelled. *Nature* **437**, 1376-1380.

Dorey, K. and Amaya, E. (2010). FGF signalling: diverse roles during early vertebrate embryogenesis. *Development* **137**, 3731-3742.

Fletcher, R. B. and Harland, R. M. (2008). The role of FGF signaling in the establishment and maintenance of mesodermal gene expression in Xenopus. *Dev Dyn* **237**, 1243-1254.

Garcia-Garcia, M. J. and Anderson, K. V. (2003). Essential role of glycosaminoglycans in Fgf signaling during mouse gastrulation. *Cell* **114**, 727-737.

Hao, H. X., Xie, Y., Zhang, Y., Charlat, O., Oster, E., Avello, M., Lei, H., Mickanin, C., Liu, D., Ruffner, H., et al. (2012). ZNRF3 promotes Wnt receptor turnover in an R-spondin-sensitive manner. *Nature* **485**, 195-200.

Harland, R. M. (1991). *In situ* hybridization: an improved whole-mount method for *Xenopus* embryos. In *Methods Cell Biol.* (ed. B. K. Kay & H. B. Peng), pp. 685-695. San Diego: Academic Press Inc.

Heasman, J., Kofron, M. and Wylie, C. (2000). Beta-catenin signaling activity dissected in the early Xenopus embryo: a novel antisense approach. *Dev Biol* **222**, 124-134.

Itoh, K., Brott, B. K., Bae, G. U., Ratcliffe, M. J. and Sokol, S. Y. (2005). Nuclear localization is required for Dishevelled function in Wnt/beta-catenin signaling. *J Biol* **4**, 3.

Itoh, K. and Sokol, S. Y. (1994). Heparan sulfate proteoglycans are required for mesoderm formation in Xenopus embryos. *Development* **120**, 2703-2711.

Jin, Y. R. and Yoon, J. K. (2012). The R-spondin family of proteins: emerging regulators of WNT signaling. *Int J Biochem Cell Biol* **44**, 2278-2287.

Kazanskaya, O., Glinka, A., del Barco Barrantes, I., Stannek, P., Niehrs, C. and Wu, W. (2004). R-Spondin2 is a secreted activator of Wnt/beta-catenin signaling and is required for Xenopus myogenesis. *Dev Cell* **7**, 525-534.

Kim, K. A., Kakitani, M., Zhao, J., Oshima, T., Tang, T., Binnerts, M., Liu, Y., Boyle, B., Park, E., Emtage, P., et al. (2005). Mitogenic influence of human R-spondin1 on the intestinal epithelium. *Science* **309**, 1256-1259.

Kim, K. A., Zhao, J., Andarmani, S., Kakitani, M., Oshima, T., Binnerts, M. E., Abo, A., Tomizuka, K. and Funk, W. D. (2006). R-Spondin proteins: a novel link to beta-catenin activation. *Cell Cycle* **5**, 23-26.

Kimelman, D. and Kirschner, M. (1987). Synergistic induction of mesoderm by FGF and TGF-beta and the identification of an mRNA coding for FGF in the early Xenopus embryo. *Cell* **51**, 869-877.

Koo, B. K., Spit, M., Jordens, I., Low, T. Y., Stange, D. E., van de Wetering, M., van Es, J. H., Mohammed, S., Heck, A. J., Maurice, M. M., et al. (2012). Tumour suppressor RNF43 is a stem-cell E3 ligase that induces endocytosis of Wnt receptors. *Nature* **488**, 665-669.

LaBonne, C., Burke, B. and Whitman, M. (1995). Role of MAP kinase in mesoderm induction and axial patterning during Xenopus development. *Development* **121**, 1475-1486.

Lowther, W., Wiley, K., Smith, G. H. and Callahan, R. (2005). A new common integration site, Int7, for the mouse mammary tumor virus in mouse mammary tumors identifies a gene whose product has furin-like and thrombospondin-like sequences. *J Virol* **79**, 10093-10096.

Mohammadi, M., McMahon, G., Sun, L., Tang, C., Hirth, P., Yeh, B. K., Hubbard, S. R. and Schlessinger, J. (1997). Structures of the tyrosine kinase domain of fibroblast growth factor receptor in complex with inhibitors. *Science* **276**, 955-960.

Nam, J. S., Park, E., Turcotte, T. J., Palencia, S., Zhan, X., Lee, J., Yun, K., Funk, W. D. and Yoon, J. K. (2007). Mouse R-spondin2 is required for apical ectodermal ridge maintenance in the hindlimb. *Dev Biol* **311**, 124-135.

Nieuwkoop, P. D. and Faber, J. (1967). *Normal Table of Xenopus laevis (Daudin)*. Amsterdam: North Holland.

Northrop, J. L. and Kimelman, D. (1994). Dorsal-ventral differences in Xcad-3 expression in response to FGF-mediated induction in Xenopus. *Dev Biol* **161**, 490-503.

Ohkawara, B., Glinka, A. and Niehrs, C. (2011). Rspo3 binds syndecan 4 and induces Wnt/PCP signaling via clathrin-mediated endocytosis to promote morphogenesis. *Dev Cell* **20**, 303-314.

Ornitz, D. M. and Itoh, N. (2015). The Fibroblast Growth Factor signaling pathway. *Wiley Interdiscip Rev Dev Biol* **4**, 215-266.

Patel, A. L. and Shvartsman, S. Y. (2018). Outstanding questions in developmental ERK signaling. *Development* **145**.

Peng, H. B. (1991). Xenopus laevis: Practical uses in cell and molecular biology. Solutions and protocols. *Methods Cell Biol* **36**, 657-662.

Rapraeger, A. C., Krufka, A. and Olwin, B. B. (1991). Requirement of heparan sulfate for bFGF-mediated fibroblast growth and myoblast differentiation. *Science* **252**, 1705-1708.

Raslan, A. A. and Yoon, J. K. (2019). R-spondins: Multi-mode WNT signaling regulators in adult stem cells. *Int J Biochem Cell Biol* **106**, 26-34.

Sato, T., Vries, R. G., Snippert, H. J., van de Wetering, M., Barker, N., Stange, D. E., van Es, J. H., Abo, A., Kujala, P., Peters, P. J., et al. (2009). Single Lgr5 stem cells build crypt-villus structures in vitro without a mesenchymal niche. *Nature* **459**, 262-265.

Seshagiri, S., Stawiski, E. W., Durinck, S., Modrusan, Z., Storm, E. E., Conboy, C. B., Chaudhuri, S., Guan, Y., Janakiraman, V., Jaiswal, B. S., et al. (2012). Recurrent R-spondin fusions in colon cancer. *Nature* **488**, 660-664.

Slack, J. M., Darlington, B. G., Heath, J. K. and Godsave, S. F. (1987). Mesoderm induction in early Xenopus embryos by heparin-binding growth factors. *Nature* **326**, 197-200.

Smith, J. C., Price, B. M., Green, J. B., Weigel, D. and Herrmann, B. G. (1991). Expression of a Xenopus homolog of Brachyury (T) is an immediate-early response to mesoderm induction. *Cell* **67**, 79-87.

Taniguchi, K., Ayada, T., Ichiyama, K., Kohno, R., Yonemitsu, Y., Minami, Y., Kikuchi, A., Maehara, Y. and Yoshimura, A. (2007). Sprouty2 and Sprouty4 are essential for embryonic morphogenesis and regulation of FGF signaling. *Biochem Biophys Res Commun* **352**, 896-902.

Tatsumi, Y., Takeda, M., Matsuda, M., Suzuki, T. and Yokoi, H. (2014). TALEN-mediated mutagenesis in zebrafish reveals a role for r-spondin 2 in fin ray and vertebral development. *FEBS Lett* **588**, 4543-4550.

Theodorou, V., Kimm, M. A., Boer, M., Wessels, L., Theelen, W., Jonkers, J. and Hilkens, J. (2007). MMTV insertional mutagenesis identifies genes, gene families and pathways involved in mammary cancer. *Nat Genet* **39**, 759-769.

Turner, N. and Grose, R. (2010). Fibroblast growth factor signalling: from development to cancer. *Nat Rev Cancer* **10**, 116-129.

Umbhauer, M., Marshall, C. J., Mason, C. S., Old, R. W. and Smith, J. C. (1995). Mesoderm induction in Xenopus caused by activation of MAP kinase. *Nature* **376**, 58-62.

Wittler, L., Shin, E. H., Grote, P., Kispert, A., Beckers, A., Gossler, A., Werber, M. and Herrmann, B. G. (2007). Expression of Msgn1 in the presomitic mesoderm is controlled by synergism of WNT signalling and Tbx6. *EMBO Rep* **8**, 784-789.

Yamada, W., Nagao, K., Horikoshi, K., Fujikura, A., Ikeda, E., Inagaki, Y., Kakitani, M., Tomizuka, K., Miyazaki, H., Suda, T., et al. (2009). Craniofacial malformation in R-spondin2 knockout mice. *Biochem Biophys Res Commun* **381**, 453-458.

Yayon, A., Klagsbrun, M., Esko, J. D., Leder, P. and Ornitz, D. M. (1991). Cell surface, heparin-like molecules are required for binding of basic fibroblast growth factor to its high affinity receptor. *Cell* **64**, 841-848.

Zhang, M., Zhang, P., Liu, Y., Lv, L., Zhang, X., Liu, H. and Zhou, Y. (2017). RSPO3-LGR4 Regulates Osteogenic Differentiation Of Human Adipose-Derived Stem Cells Via ERK/FGF Signalling. *Sci Rep* **7**, 42841.

Figures
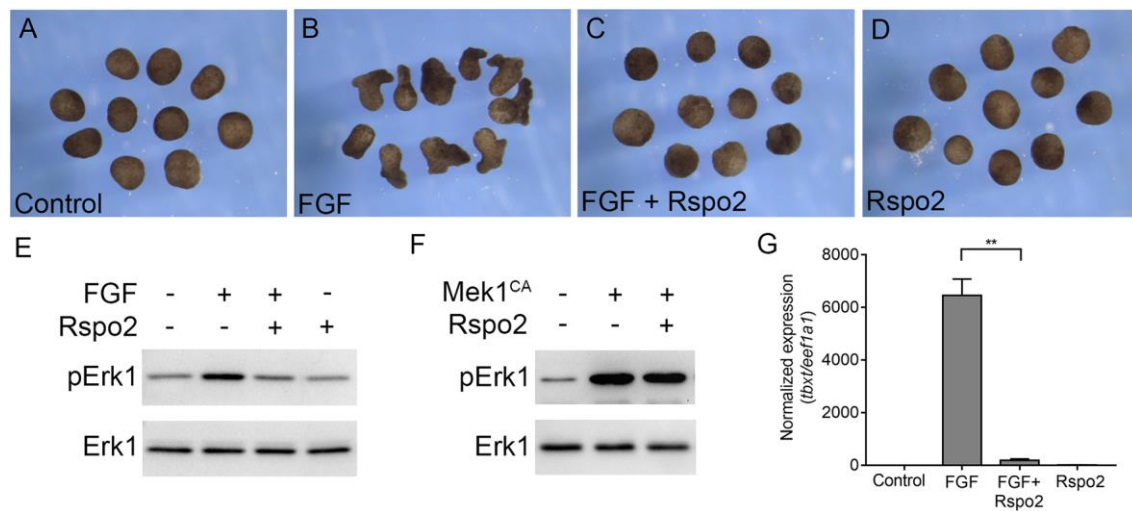
Fig. 1. Rspo2 inhibits ectoderm response to FGF but not MEK1. Four-cell stage embryos were injected animally with Rspo2 RNA (0.5 ng) and Mek1^{CA} RNA (12 pg) as indicated. Ectoderm explants were dissected at stage 8 and treated with 100 ng/ml FGF2 protein. When control embryos reached stage 13, the explant morphology was imaged (A-D) or they were lysed for immunoblot or RT-qPCR analysis (E-G). A, control uninjected ectoderm explants; B, FGF-treated explants; C, Rspo2-expressing explants stimulated with FGF; D, Rspo2-expressing explants. Ten ectoderm explants were used per group in each experiment, the experiments have been repeated 5 times. E-F, Modulation of Erk1 activation by Rspo2. Immunoblotting was carried out with the antibodies against pErk1 and total Erk1. Data represent 3-5 independent experiments. G, Rspo2 inhibits FGF-dependent induction of *tbxt*. RT-qPCR analysis was performed for *tbxt* and normalized by *eef1a1*. The graph shows a representative experiment with triplicate samples from three independent experiments. Means +/- s. d. are shown. Statistical significance was assessed by Students t-test **, p<0.05.
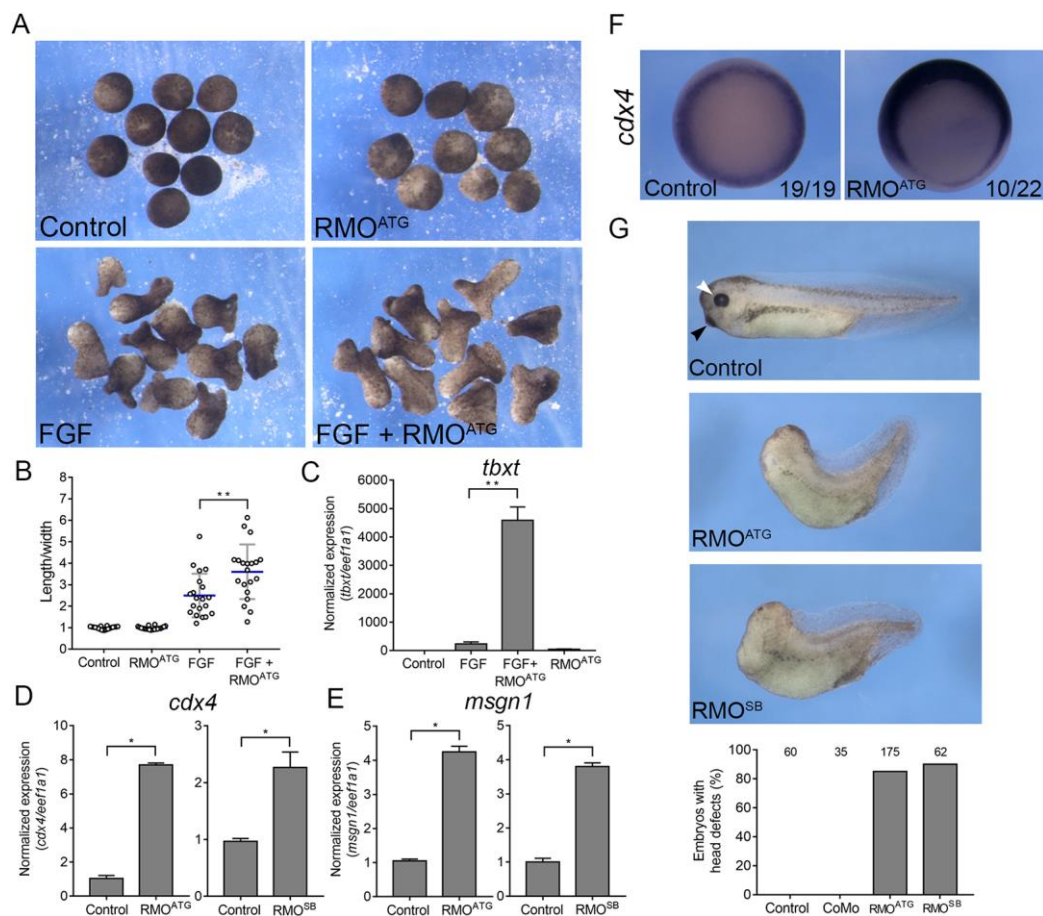
Fig. 2. Rspo2 depletion promotes FGF signaling. A, B, Two-cell embryos were injected animally with RspoMO^{ATG} (10 ng) or RspoMO^{SB} (20 ng). Ectoderm explants were dissected at stage 8, treated with 25 ng/ml of FGF2 and cultured until stage 13. A, Representative morphology is shown. B, Quantification of the data in A, representative of two independent experiments. C, RT-qPCR shows enhanced *tbxt* expression in FGF-stimulated ectodermal explants (stage 13) after Rspo2 depletion. D-E, Enhanced *cdx4* and *msgn1* expression in dorsal marginal zone (DMZ) explants depleted of Rspo2. RT-qPCR was carried out in stage 13 DMZ explants that were isolated at stage 10. Means +/- s. d. are shown for triplicate samples. Graphs are representative of three independent experiments. F, *In situ* hybridization with anti-sense *cdx4* probes was carried out with stage 10+ control embryos and embryos injected marginally four times with 10 ng of RspoMO^{ATG}. The

number of embryos with the displayed phenotype and the total number of injected embryos are shown. G, Two dorsal animal blastomeres of four-cell embryos were injected with RMO^{ATG} or RMO^{SB} (10-20 ng each). Representative embryos are shown at stage 39. Arrowheads point to the eye (white) and the cement gland (black). The graph presents frequencies of embryos with head defects (missing eyes, cement gland and reduced facial structures). Numbers of embryos per group are shown on the top of each bar. Data are representative of 3 to 4 independent experiments. **, *, p<0.05, Student's t-test.
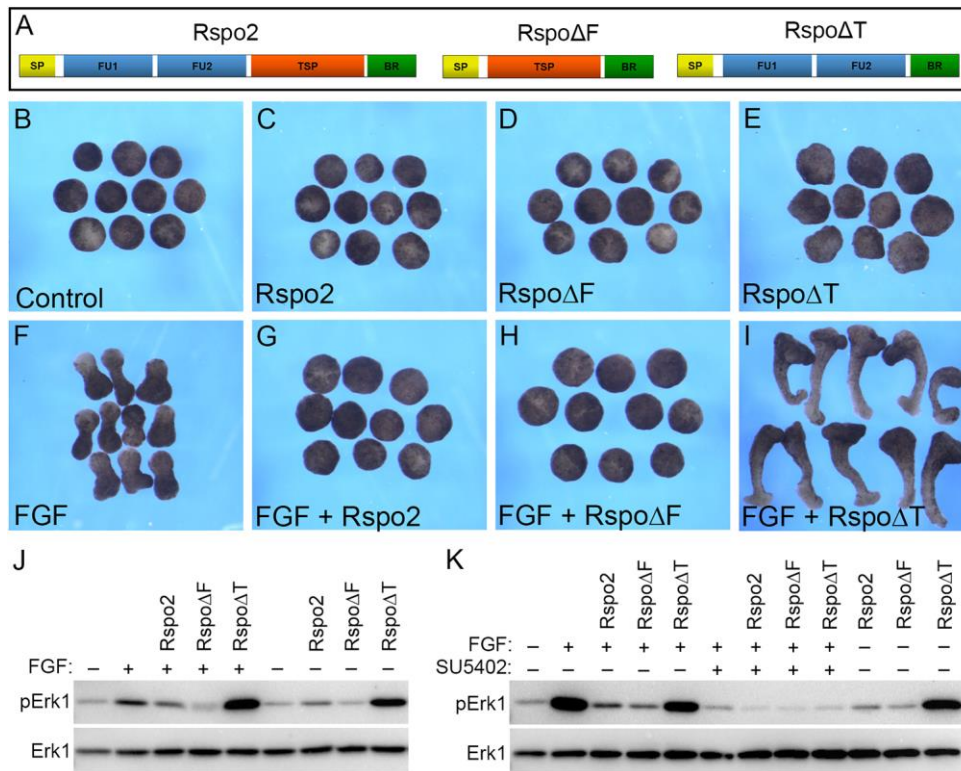
Fig. 3. Mapping FGF inhibitory activity to the TSP domain. A, Schematic of different Rspo2 constructs. B-K, Four-cell embryos were injected with Rspo2, RspoΔF, or RspoΔT RNA, 0.5 ng each, as indicated, and cultured until stage 8. Ectoderm explants were dissected, treated with 100 ng/ml of FGF2 with or without SU5402 (100 μM, final concentration) and cultured until stage 13. B-I, Explant morphology is shown for unstimulated explants (B-E) and after FGF2 stimulation (F-I). J, K, Effects of Rspo2 constructs on FGF-dependent Erk1 activation. Immunoblot analysis was carried out with the antibodies against pErk1 and total Erk1.
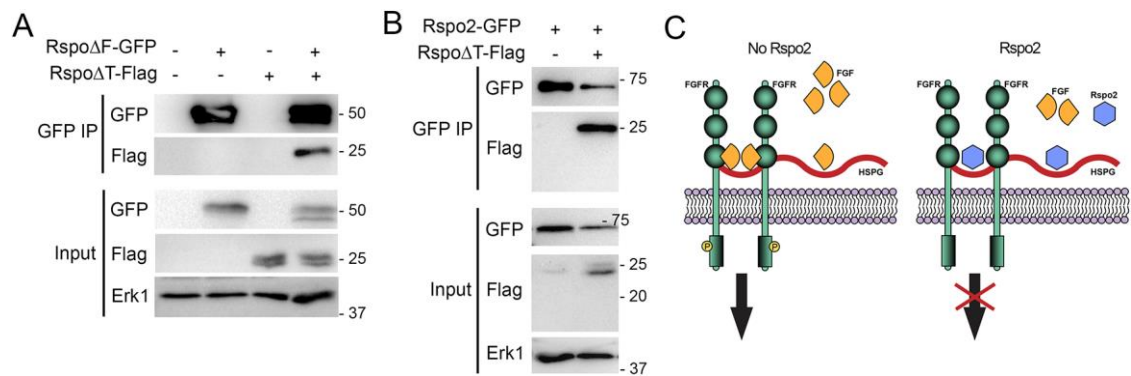
Fig. 4. The intramolecular interaction of protein domains in Rspo2. Four-cell stage embryos were injected RspoΔF-GFP, RspoΔT-Flag alone or coinjected. The embryos were cultured until stage 12 and lysed for GFP pulldown. A, RspoΔT-Flag is co-immunoprecipitated by RspoΔF-GFP. B, RspoΔT-Flag is co-immunoprecipitated by Rspo2-GFP. C, Putative mechanistic model of FGF pathway inhibition by Rspo2. The association of Rspo2 with HSPGs prevents FGF ligand binding and signaling.

Supplementary Material

Supplementary Figures S1-S4.
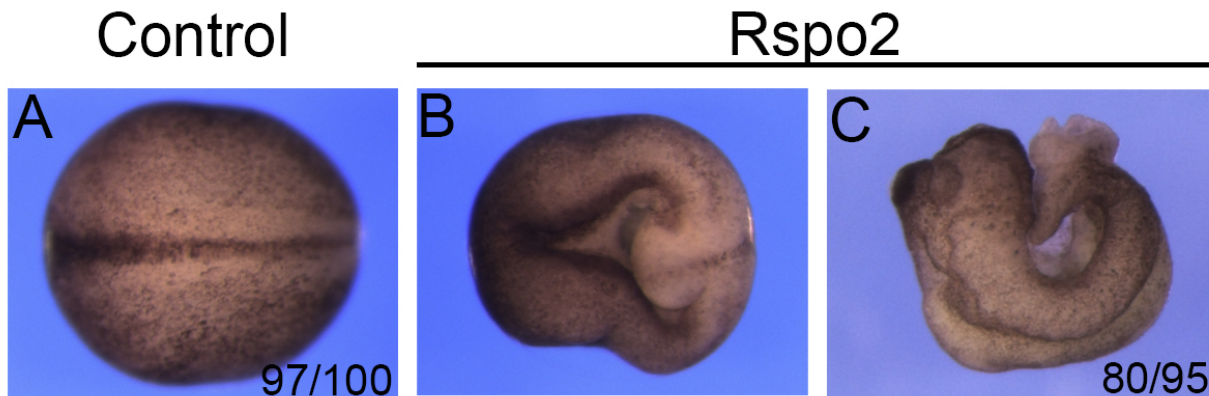
**Fig. S1. Phenotypes of embryos injected with Rspo2 RNA.**

Four-cell stage embryos were injected into two dorsal blastomeres with Rspo2 RNA (0.5 ng) and allowed to develop until neurula (A, B) or tailbud (C) stages. (A) Uninjected control embryo, stage 19. (B-C) Rspo2-expressing embryos. Open blastopore and posterior defects are apparent. Representative embryos are shown, with more than 20 embryos per group from 5 separate experiments. The number of embryos displaying the phenotype and the total number of embryos are indicated.
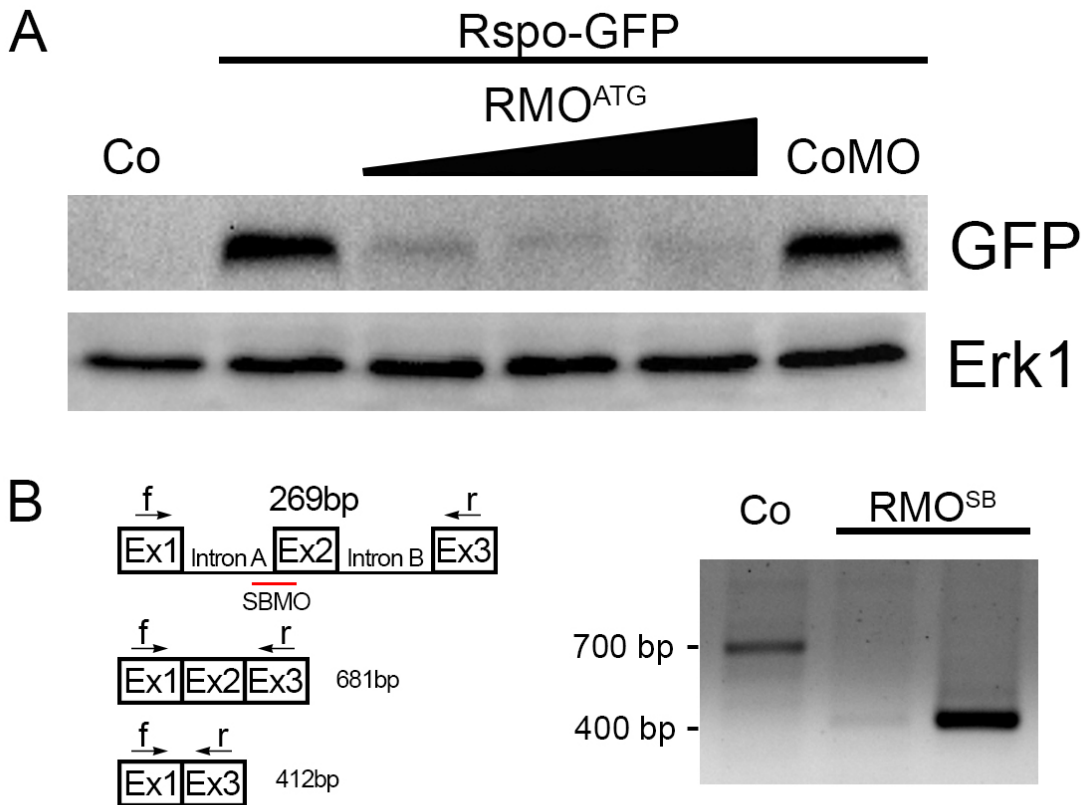
Fig. S2. Validation of Rspo2 knockdown *in vivo*. A, Embryos were injected with Rspo2-GFP RNA (500 pg) alone or coinjected with increasing amounts of RspoMO^{ATG} (10, 20, and 30 ng). Lysates were prepared from injected embryos at stage 11 for immunoblotting with anti-GFP antibody. CoMO (control MO). Co, control uninjected embryo. Erk1 is a control for loading. B, Schematic of RT-PCR to detect changes in Rspo2 RNA splicing. The PCR fragment of 681 b. p. corresponds to three exons expected in a control embryo. The 412 bp DNA fragment is expected for Rspo2.L RNA with un-spliced exon 2. RT-PCR was carried out with RNA prepared from stage 11 embryos previously injected with RspoMO^{SB} (20 ng). PCR fragments corresponding to a control embryo (Co) and two different embryos injected with RspoMO^{SB} are shown.
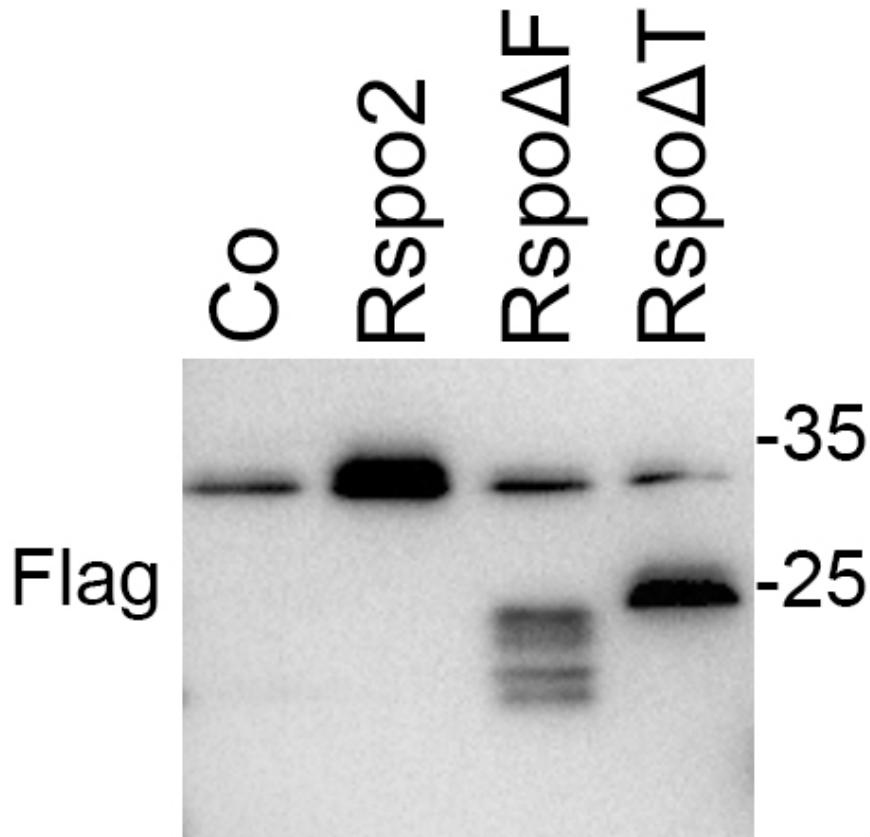
Fig. S3. Expression levels of Rspo2 constructs. RNAs encoding different Flag-tagged Rspo2 constructs (see Fig. 3A) were injected into four cell embryos, ectoderm explants were isolated at midblastula stages and cultured until stage 11 for immunoblotting with anti-Flag antibody.
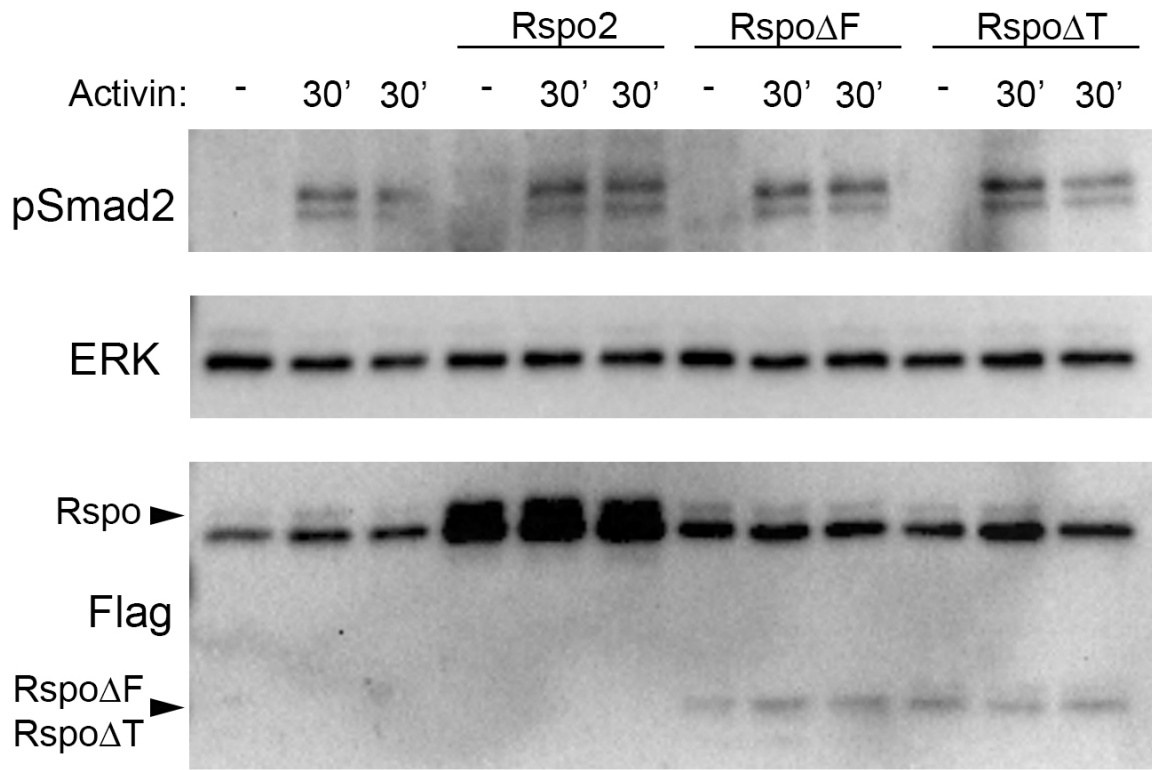
Fig. S4. Lack of Rspo2 effects on Activin/Nodal signaling. RNAs encoding different Flag-tagged Rspo2 constructs were injected into four cell embryos, ectoderm explants were isolated at midblastula stages and stimulated with 0.5 ng/ml of Activin A for 30'. Cell lysates were separated by PAGE and immunoblotted with anti-phospho-Smad2 and anti-Flag antibody.

Table S1.

Primers for Rspo2 mutagenesis
RspoΔF:
5'- AGACGGAGCAAGAGAGCCAGATCTCCATTGGATGACACCATG-3'
RspoΔT:
5'-TGCGTGGATGGCTGTGAAGCTAGCGGAGGAACAAGAACCACA-3'

Primers for RT-qPCR

cdx4.L:	Forward: 5'-TGATTTATCACCTAACCAG-3'
	Reverse: 5'-GTCCCAGATGGATGAGGAGA-3'
eef1a1.S:	Forward: 5'-ACCCTCCTCTTGGTCGTTTT-3'
	Reverse: 5'-TTTGGTTTTCGCTGCTTTCT-3'
tbxt.S:	Forward: 5'-TCACTAGCCATTCATTCCCT-3'
	Reverse: 5'-GACTATCGATTCCCTCATCC -3'
msgn1.L	Forward: 5'-GTATCCAACACTTTGCCATG-3'
	Reverse: 5'-AGCACTGGAGAAGGTTTGTG-3'